Excited state intermolecular proton transfer in isolated clusters: 1-naphthol/ammonia and water

Seong K. Kim, Shijian Li, and Elliot R. Bernstein

Excited state intermolecular proton transfer in isolated clusters: 1-naphthol/ammonia and water

Seong K. Kim,[a] Shijian Li, and Elliot R. Bernstein
*Colorado State University, Chemistry Department, Fort Collins, Colorado 80523*

The excited singlet state intermolecular proton transfer reaction in jet-cooled clusters of 1-naphthol/ammonia and water is investigated employing mass resolved excitation, threshold photoionization, and emission spectroscopy. The complete data set indicates that no proton transfer occurs for 1-naphthol$(NH_3)_{1,2}$ and $(H_2O)_n$, $n = 1,...,20$ clusters. Proton transfer occurs for (at least) one configuration of the 1-naphthol$(NH_3)_3$ cluster, as well as all 1-naphthol$(NH_3)_n$, $n \geqslant 4$, clusters. The (at least) two configurations of 1-naphthol$(NH_3)_3$ clusters are distinguished by threshold photoionization studies. The 1-naphthol$(NH_3)_3$ cluster for which proton transfer is indicated has a threshold photoionization energy ~ 2000 cm^{-1} below the other 1-naphthol$(NH_3)_3$ cluster configurations. These results are employed to explain the previous discrepancy between static spectroscopic experiments and picosecond time resolved dynamic experiments concerning proton transfer in the 1-naphthol$(NH_3)_3$ cluster. Calculations of cluster geometry in 1-naphthol/ammonia and water cluster systems suggest some qualitative explanations of these observations.

I. INTRODUCTION

Proton transfer reactions are one of the elementary chemical reactions that play an important role in numerous chemical and biological processes. Photoinduced proton transfer reactions are also ubiquitous in chemistry and biology and offer the added advantage of ready access for kinetic and mechanistic studies.[1] Photoinduction allows the experimenter to initiate the reaction and thus the mechanistic sequence can be followed with time at a point of his choosing. One of the major issues for reactions of any sort, and elementary reactions (i.e., proton transfers and electron transfers) in particular, is the role of the solvent in the reaction mechanism and kinetics. One can study the role played by the solvent in such reactions by controlling its presence in the reacting system. This can be accomplished in a number of instances through the study of chemical reactions in small solute/solvent clusters of known size and often geometry, as generated in a supersonic expansion.[2] The clusters may then be accessed by optical and mass spectroscopy and the reaction studied as a function of many separate cluster parameters.

Almost all excited state proton transfer chemical reactions in large molecules or clusters that have been investigated are of the form

$$(AH)B_n \xrightarrow[h\nu]{} (AH)^* B_n \rightarrow A^{*-}(HB_n)^+. \qquad (1)$$
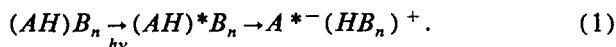
In these cases the requirements for the excited state proton transfer reaction in the cluster are as follows: (1) the chromophore solute (AH) must be a good acid in the excited state (small pK_a in S_1) and a poor acid in the ground state (large pK_a in S_0)—the concomitant change in pK_a upon excitation can be estimated by a Förster cycle calculation[3,4]; (2) AH must have relatively high vapor pressure and a strong $S_1 \leftarrow S_0$ transition; and (3) the solvent (cluster) B_n must have a large proton affinity.

A number of systems of this nature has been investigated by supersonic expansion optical/mass spectroscopy techniques: convincing evidence has been presented for 1-naphthol/ammonia[5-8] and piperidine;[7,8] 2-naphthol/ammonia;[9] phenol/ammonia[10,11] and ethylamine,[12] hydroxypyridine/pyridone/ammonia;[13] and an intramolecular proton transfer in 2,5-bis(2-benzoxazolyl)hydroquinone.[14] We will shortly publish our proton transfer findings for 2-substituted phenols (allyl, propenyl, propyl) clustered with ammonia and water.[15]

The general questions one hopes to answer with such studies of cold clusters are the following: (1) what is the mechanism for the excited state proton transfer? (2) will knowledge of this mechanism aid in the understanding of solution phase behavior? (3) what is the critical number of solvent molecules in the cluster for which the excited state proton transfer is induced? (4) what determines this critical number? (5) how important is specific cluster and solvent geometry for the reaction?

Several recent studies[5-12] have placed emphasis on the critical cluster size (i.e., the number n of solvent molecules) for which intermolecular proton transfer is induced. In general, a number of spectroscopic observations can be employed to suggest that proton transfer reactions have occurred in clusters. First, the excitation spectrum can be broad due to coupling of the S_1 state of the chromophore to the high density of product states and/or to a reduced lifetime for the unreacted cluster states. Second, red shifted emission can arise from the product state $A^{*-}(HB_n)^+$ in addition to or instead of the normal reactant $AH^*(B_n)$ emission. Third, a red shift in the ionization threshold is expected upon proton transfer in S_1 because the product $A^{*-}(HB_n)^+$ has stabilized separated charges and thus should ionize at lower energy. Fourth, dynamical behavior can be associated with any and all of the changes—it can be followed with time resolved spectroscopic techniques. Figure 1(a) represents the potential curves and electronic transitions that might give rise to such behavior assuming $n = 3$

[a] Current address: Code 6546, Naval Research Laboratory, Washington, D.C. 20375-5000.
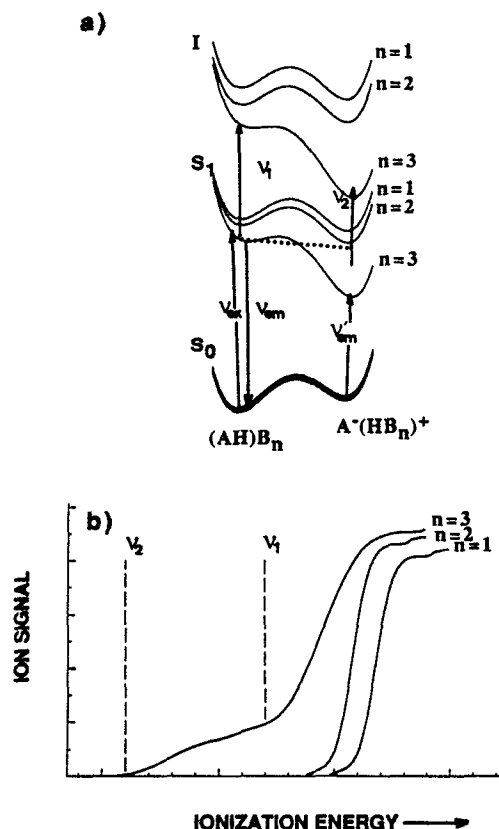
FIG. 1.(a) The expected curves for the excited state proton transfer in $(AH)B_n$ systems. In this example, $n = 3$ is the critical number of B solvent molecules for proton transfer. The symbols ν_{em} and ν'_{em} stand for the normal and proton transfer emission, respectively, and ν_1 and ν_2 are the normal and proton transfer $I \leftarrow S_1$ transition energies, respectively. ν_{ex} is the normal excitation $S_1 \leftarrow S_0$ energy. (b) The expected threshold photoionization spectra for the corresponding system. The successive red shifts in the ionization thresholds upon additional clustering are due to the binding energy increases in the ionization state. Much larger red shift in the ionization threshold is expected for $n = 3$ due to the separation of the charges in the product. The ionization transitions ν_1 and ν_2 are indicated for $n = 3$.

is the critical cluster solvent size for the proton transfer reaction.

None of the above harbingers of proton transfer in clusters is without its own complications, however. Broadening of the excitation features can be caused by contributions from spectral congestion due to other clusters or the inhomogeneous broadening from the clusters' own density of states. The emission spectra are of necessity always obtained without mass resolution and thus the exact value of critical cluster size cannot be obtained definitively based only on emission studies. Threshold photoionization does yield mass information; but the red shift that occurs upon cluster size increase due to differential increased binding in the ionic cluster compared to the neutral cluster and changes in Franck–Condon factors for ionization can obscure the ionization changes associated with internal cluster charge separation [Fig. 1(b)]. Three photon ionization processes can also interfere with expected two photon trends.[16] Time resolved spectroscopy (emission and mass resolved) may be the ultimate tool for these determinations, but even this method of detection for proton transfer relies on a precise

analysis of the steady state spectra. One is forced to conclude that only a combination of these many techniques will yield a reliable indication that proton transfer (chemical reaction) has occurred for a particular cluster in the S_1 excited electronic state.

Recently, picosecond pump/probe experiments employing mass selective detection were reported for jet-cooled 1-naphthol[8] and phenol[11] clustered with water and ammonia. The reported observations for water clusters are in agreement with the steady state results:[6,17] no proton transfer occurs even for $n > 20$. Agreement between static and dynamic measurements for 1-naphthol(piperidine)$_n$ clusters is also good: $n \geqslant 2$ induces the S_1 transfer of a proton.[8,9] Agreement on the critical size for excited state proton transfer in 1-naphthol/ammonia clusters and phenol/ammonia clusters is not good, however. Static spectra (emission) of 1-naphthol/ammonia clusters suggest transfer occurs at $n = 4$,[6] while dynamic results suggest $n = 3$ clusters[8] induce transfer. Static threshold ionization results for phenol/ammonia clusters suggest proton transfer in $n = 4$ clusters[10] while the dynamic results[11] lead to the conclusion that transfer occurs only at $n = 5$ phenol/ammonia clusters.

In this report we discuss and emphasize mass resolved excitation spectra and threshold photoionization data for 1-naphthol/ammonia and water clusters as a function of cluster size (solvent number n). We find that not only does excited state (S_1) proton transfer depend on the number of solvent molecules present in the cluster, but it also apparently is a function of the cluster structure. One cluster of 1-naphthol(NH_3)$_3$ has a very low ionization energy threshold (equal to that of $n = 4$ clusters) and we suggest that this cluster, due to a particularly advantageous solvation structure, induces excited state proton transfer while other $n = 3$ clusters do not. Excited state proton transfer apparently occurs for all 1-naphthol(NH_3)$_n$ clusters for $n \geqslant 4$. This conclusion rationalizes the static and dynamic data for the 1-naphthol/ammonia proton transfer system.[5–8] We attempt to understand these results in terms of trends in cluster structures calculated with a standard intermolecular potential energy function and an energy minimization algorithm.

II. EXPERIMENTAL PROCEDURES

One-color and two-color mass resolved excitation spectra of 1-naphthol and its clusters with water and ammonia are obtained in the usual manner.[18] The laser systems consist of Nd/YAG pumped dye lasers whose independently tunable outputs are doubled or mixed with residual 1.064 μm light to match the $S_1 \leftarrow S_0$ and $I \leftarrow S_1$ transitions of the appropriate clusters of interest.

1-naphthol is purchased from Aldrich Chemical Co. and placed in a heated pulsed nozzle at 65 °C.

Intensity of the ionization laser is monitored and maintained between 300 and 1000 μJ/pulse. The energy of the $S_1 \leftarrow S_0$ excitation pulse is attenuated to $\sim 2\,\mu$J for 1-naphthol(NH_3)$_1$, 20 μJ for 1-naphthol(NH_3)$_2$ and (H_2O)$_1$, 50 μJ for 1-naphthol(NH_3)$_3$, and 150 μJ for 1-naphthol(NH_3)$_4$ cluster studies. Since the threshold is broad for these clusters, we simply take the wavelength at which photoionization current disappears for the threshold. The thresholds

reported are for extraction electric fields of ~ 100 V/cm.

Dispersed (wavelength resolved) emission and wavelength resolved fluorescence excitation spectra are obtained by the use of UV cutoff filters (Hoya U34, U36, L38, L40) placed in front of the photo tube.

Calculations of cluster geometries are accomplished as we have previously reported.[13] Molecules (solute and solvent) are randomly placed in a box of chosen size and an energy minimization algorithm finds the lowest energy local geometry for the molecules. The calculations are repeated many times to find all the possible local energy minima on the potential surface.

The interaction energy between the molecules of the cluster for a given geometry is calculated based on a potential energy function containing coulomb, hydrogen bonding (when appropriate), and Lennard-Jones atom–atom terms.[19]

Geometries and point charge distributions for both the solute and solvent are obtained from MOPAC 5/PM3 calculations[20] prior to the potential energy minimization.

RESULTS

A. Mass resolved excitation spectroscopy

The mass resolved excitation spectra of 1-naphthol and some of its clusters with ammonia and water are presented in Fig. 2. The bare molecule electronic origin is located at $31\ 458$ cm^{-1}. This feature has been suggested to arise from the anti-1-naphthol conformer[21-23] indicated in Scheme I. In our experiment the syn isomer has only negligible population (origin at $31\ 182$ cm^{-1}) and therefore no significant effort has been made to obtain its cluster spectra.

Scheme I

1-Naphthol

Anti   Syn
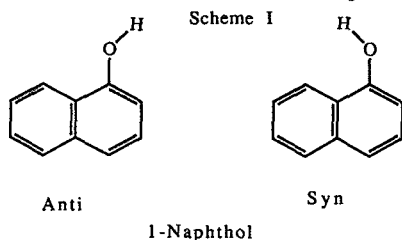
As the 1-naphthol/water clusters become larger, $1 \leqslant n \leqslant 7$, the spectra become broader with a few sharp features appearing above a broad background.[17]

The clusters of 1-naphthol with ammonia appear to have somewhat different mass resolved excitation spectra than those found with water (Fig. 2). The 1-naphthol(NH_3)$_1$ cluster apparently shows a single origin feature at $31\ 220$ cm^{-1}. Multiple features are observed for the 1-naphthol(NH_3)$_2$ clusters probably due to both different cluster conformations and van der Waals mode intensity. Unlike the situation found for 1-naphthol(H_2O)$_n$, $n = 2, 3, 4,...$, no fragmentation peaks are observed for the ammonia clusters with $n = 1, 2, 3$. The 1-naphthol(NH_3)$_{4,5,...}$ clusters have red shifted, featureless, broad spectra. These findings are in complete agreement with those of previous studies.[6]

As the clusters become larger, their spectra become generally more complex and broad. To distinguish the contributions to this spectral congestion (i.e., conformers and van der Waals modes of a single species), one can compare the one-color and near threshold two-color resolved excitation
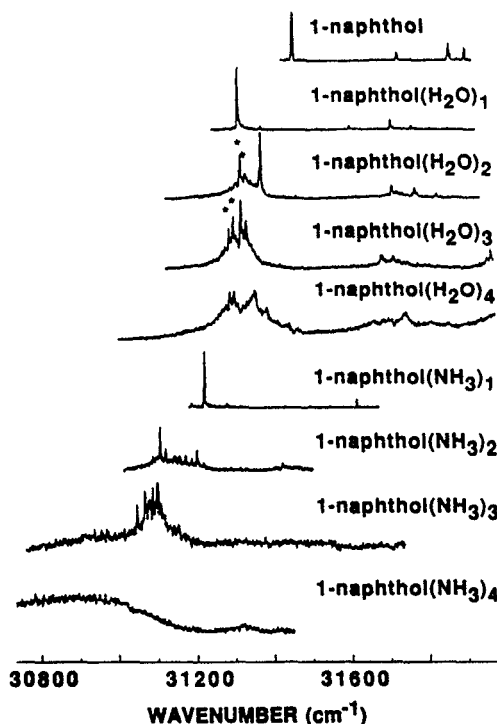

FIG. 2. One-color TOFMS of 1-naphthol and its clusters with H_2O and NH_3. Some possible fragmentation peaks are marked with *.

spectra of the various cluster masses. Such a comparison for 1-naphthol(NH_3)$_3$ is presented in Fig. 3. The possibility that many of the sharp features in the one-color spectrum of 1-naphthol(NH_3)$_3$ are due to fragmentation of higher order clusters can be eliminated because the $n \geqslant 4$ ammonia clusters do not evidence sharp features. At sufficiently low ionization energy ($\nu_{ion} \sim 26\ 500$ cm^{-1}) most of the 1-naphthol(NH_3)$_3$ intensity disappears and a "new feature" emerges at $\sim 31\ 105$ cm^{-1} which was previously obscured by more intense features from (NH_3)$_3$ clusters (of different geometry) with higher ionization energies. Figure 3 and additional
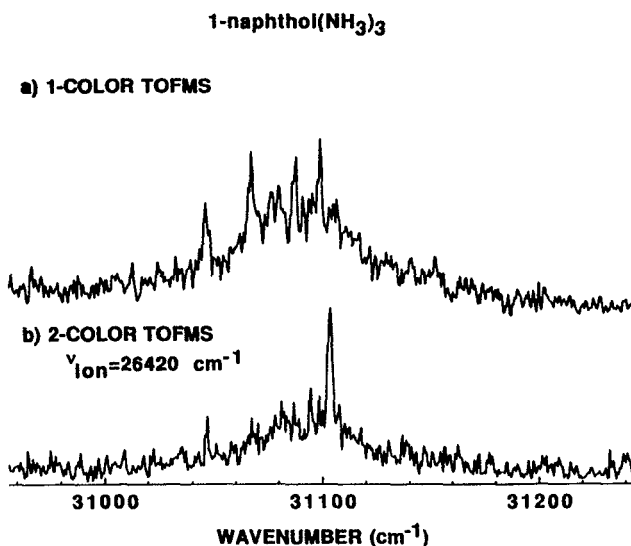

FIG. 3. (a) One-color TOFMS of 1-naphthol(NH_3)$_3$. (b) Two-color TOFMS of 1-naphthol(NH_3)$_3$. The ionization laser energy is $26\ 420$ cm^{-1}.
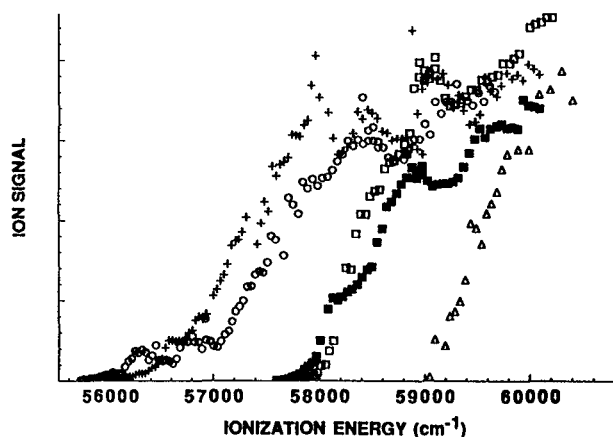
FIG. 4. The threshold photoionization spectra of 1-naphthol clusters. □: 1-naphthol(NH$_3$)$_1$ ($\nu_{ex} = 31\,221$ cm^{-1}); ■:   1-naphthol(NH$_3$)$_2$ ($\nu_{ex} = 31\,105$ cm^{-1}); +: 1-naphthol(NH$_3$)$_3$ ($\nu_{ex} = 31\,105$ cm^{-1}); O: 1-naphthol(NH$_3$)$_4$ ($\nu_{ex} = 30\,877$ cm^{-1}); △: 1-naphthol(H$_2$O)$_1$ (ν_{ex} $= 31\,310$ cm^{-1}). Excitations at 31 068, 31 077, 31 080, 31 088 cm^{-1} for other conformers of 1-naphthol(NH$_3$)$_3$ have the similar threshold photoionization behavior to 1-naphthol(NH$_3$)$_{1,2}$. Threshold photoionization of 1-naphthol(H$_2$O)$_{2,3,4}$ are similar to 1-naphthol(H$_2$O)$_1$.
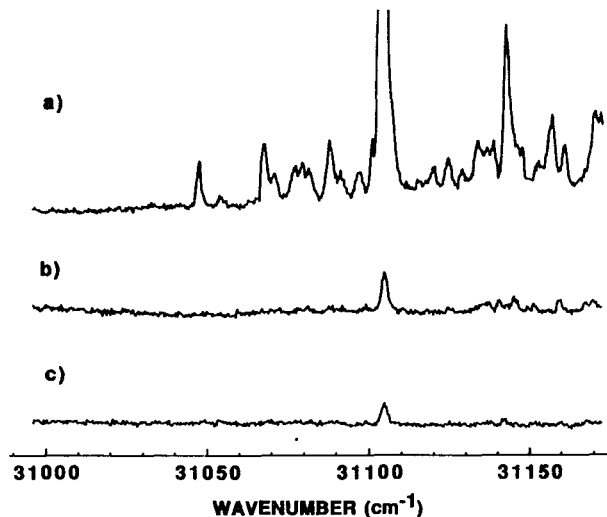

FIG. 5. Fluorescence excitation spectra for 1-naphthol/NH$_3$ with a UV34 filter (a), a UV36 filter (b), a L38 filter (c). 0.002% NH$_3$ in helium is used for expansion. Transmission of the filters are the following: UV34 (0% < 315 nm, 2.5% at 320 nm, 52% at 340 nm, 80% at 360 nm, 84% at 380 nm, 87% > 400 nm); UV36 (0% < 340 nm, 47% at 360 nm, 74% at 380 nm, 83% at 400 nm, 86% > 440 nm); L38 (0% < 355 nm, 47% at 380 nm, 78% at 400 nm, 86% at 420 nm, 90% > 460 nm).

ionization data suggest that the spectral congestion is due to contributions from many (perhaps 5 or more) 1-naphthol(NH$_3$)$_3$ cluster conformations.

B. Threshold photoionization

Figure 4 shows that the threshold photoionization intensities as a function of total ionization energy for 1-naphthol(H$_2$O)$_n$ ($n = 1, 2, 3, 4$) are quite close to one another and that they do not appear to vary systematically with n. The ionization threshold for 1-naphthol(NH$_3$)$_3$ clusters differs depending on the excitation energy in the region of the origin transition $\sim 31\,040$–31 120 cm^{-1}; that is, depending on the cluster conformer selected in the $S_1 \leftarrow S_0$ excitation. Conformers which absorb $\sim 31\,070$, 31 080, and 31 090 cm^{-1} have ionization thresholds similar to that found for 1-naphthol(NH$_3$)$_{1,2}$ clusters. The ionization potential for the conformer absorbing near 31 050 cm^{-1} is ~ 200 cm^{-1} red shifted from these latter features. In contrast, the conformer of 1-naphthol(NH$_3$)$_3$ which has an $S_1 \leftarrow S_0$ absorption $\sim 31\,105$ cm^{-1} has an ionization threshold some 1500–2000 cm^{-1} red shifted from the other conformers.

C. Wavelength resolved fluorescence excitation and dispersed (wavelength resolved) emission

Dispersed emission studies of 1-naphthol/water and ammonia clusters reveal a red shifted component ($\Delta\nu \sim 8000$ cm^{-1}) of the emission for 1-naphthol(NH$_3$)$_n$, $n \geqslant 4$,[6] but not $n = 3$. In this regard, recall that dispersed emission is obtained without mass resolution and note the $n = 3$ and 4 spectra presented in Fig. 2 for ammonia clusters. With these difficulties in mind, we have attempted to reproduce the reported dispersed emission data for 1-naphthol(NH$_3$)$_n$, $n = 1, 2, 3, 4$, clusters employing very low (0.002%) and controlled concentrations of NH$_3$ and UV

filters placed in front on the phototube. A portion of the observed, generally weak, emission is presented in Fig. 5. Figures 5(a)–5(c) show fluorescence excitation spectra about the origin regions of 1-naphthol(NH$_3$)$_{2,3}$ clusters as observed through several cutoff filters. With a UV34 filter [Fig. 5(a), see caption for transmission details—essentially transmits radiation of energy lower than 31 750 cm^{-1}, >320 nm] all the 1-naphthol(NH$_3$)$_{2,3}$ features can be observed. Note that the feature at $\sim 31\,105$ cm^{-1} should contain emission from both (NH$_3$)$_2$ and (NH$_3$)$_3$ clusters. With lower energy cutoff filters (UV36-0% transmission < 340 nm or > 29 400 cm^{-1} and L38-0% transmission < 350 nm or > 28 500 cm^{-1}), the peak at $\sim 31\,105$ cm^{-1} still persists suggesting that only red shift emission is generated by the (NH$_3$)$_3$ cluster that absorbs at this energy. Note that this feature would not be detected with a monochromator at this concentration of NH$_3$ in the expansion (f/1 vs f/8 optics).

In contrast, red shifted emission is observed from excitation of the broad features corresponding to 1-naphthol(NH$_3$)$_n$, $n \geqslant 4$. This emission could mask other red shifted emission associated with the broad absorptions for 1-naphthol(NH$_3$)$_3$ clusters (see Fig. 2).

D. Cluster structure calculations for 1-naphthol(H$_2$O)$_n$ and (NH$_3$)$_n$

One of the strong implications that arises from the spectroscopic data presented above is that for clusters of a given n value (size or mass), a number of different cluster conformation of solvent molecules with respect to the solute molecule, and, indeed, the other solvent molecules as well, can be identified. In particular, for 1-naphthol(NH$_3$)$_3$, the above data suggest that (at least) one cluster geometry supports proton transfer while others do not. Cluster geometry thus becomes an issue for the proton transfer reaction. Apparently, solvent
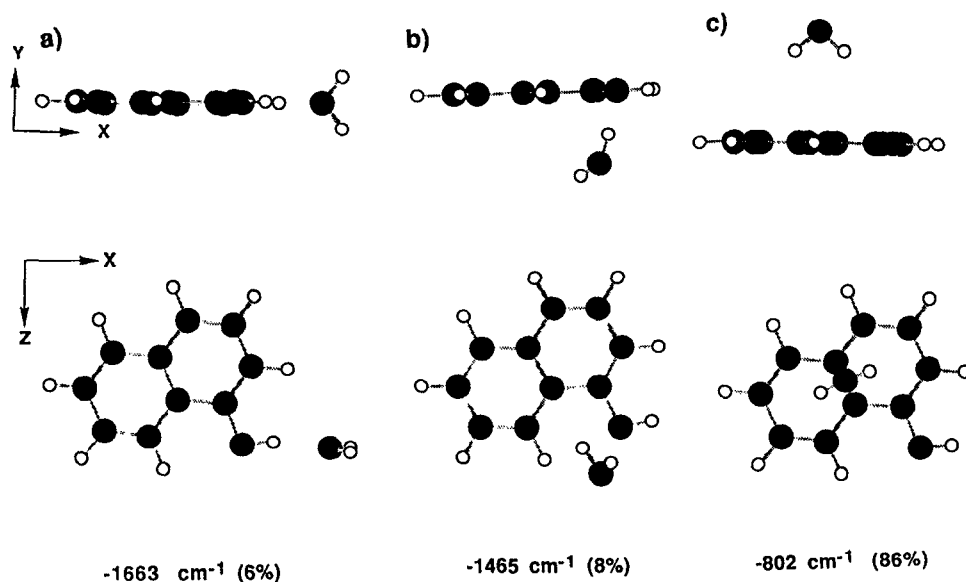
FIG. 6. Calculated geometries for 1-naphthol(H$_2$O)$_1$. The stabilization energy and the percentage of the total number of calculations resulting in the reported structure are indicated.

-1663 cm^{-1} (6%)   -1465 cm^{-1} (8%)   -802 cm^{-1} (86%)

cluster proton affinity is not the only determining factor for the reaction of Eq. (1). Thus, most likely both the resulting anion and the proton require some degree of solvation for the reaction free energy to be favorable.

1. 1-Naphthol(H$_2$O)$_1$

Three geometries are found for the 1-naphthol(H$_2$O)$_1$ cluster as shown in Fig. 6. The figure presents three different pieces of information concerning the cluster: structures, binding energy, and the frequency with which the given structure is found. This latter information is in some sense the probability for the formation of this cluster in a random encounter between solute and solvent. Thus the structures of Figs. 6(a) and 6(b) are difficult to form while that of Fig. 6(c) is easy because of the large acceptable "angle of approach" for this structure. Nonetheless, due to collisions in

the jet, the lower energy (rarer) structures are most likely the ones that actually form. The most stable structure [Fig. 6(a)] involves the naphtholic hydrogen bonded to the water oxygen. This is probably the single cluster observed in our spectrum of 1-naphthol(H$_2$O)$_1$.

2. 1-Naphthol(H$_2$O)$_{2, 3, 4}$

Many stable structures are calculated for 1-naphthol (H$_2$O)$_2$: a few of the lowest energy of these are presented in Fig. 7. For the most part, these structures involve water coordinated to the naphthol OH group and to the other water molecule present. Again these structures appear infrequently in the computer calculations but they probably dominate in the experiment due to collisional "activation" or collision induced barrier crossings on the potential surface of the forming clusters. Coordination to the π system is much less

FIG. 7. The three most stable geometries for 1-naphthol(H$_2$O)$_2$. The stabilization energy and the percentage of the total number of calculations resulting in the reported structure are indicated.

-3586 cm^{-1} (2%)   -3404 cm^{-1} (6%)   -3204 cm^{-1} (1%)

a)

b)

c)

d)

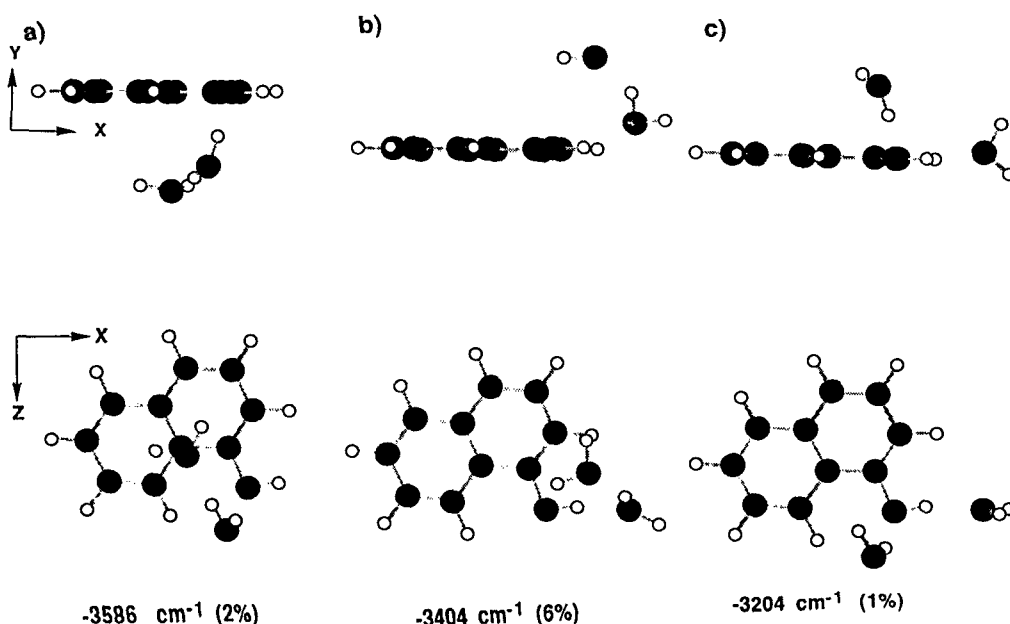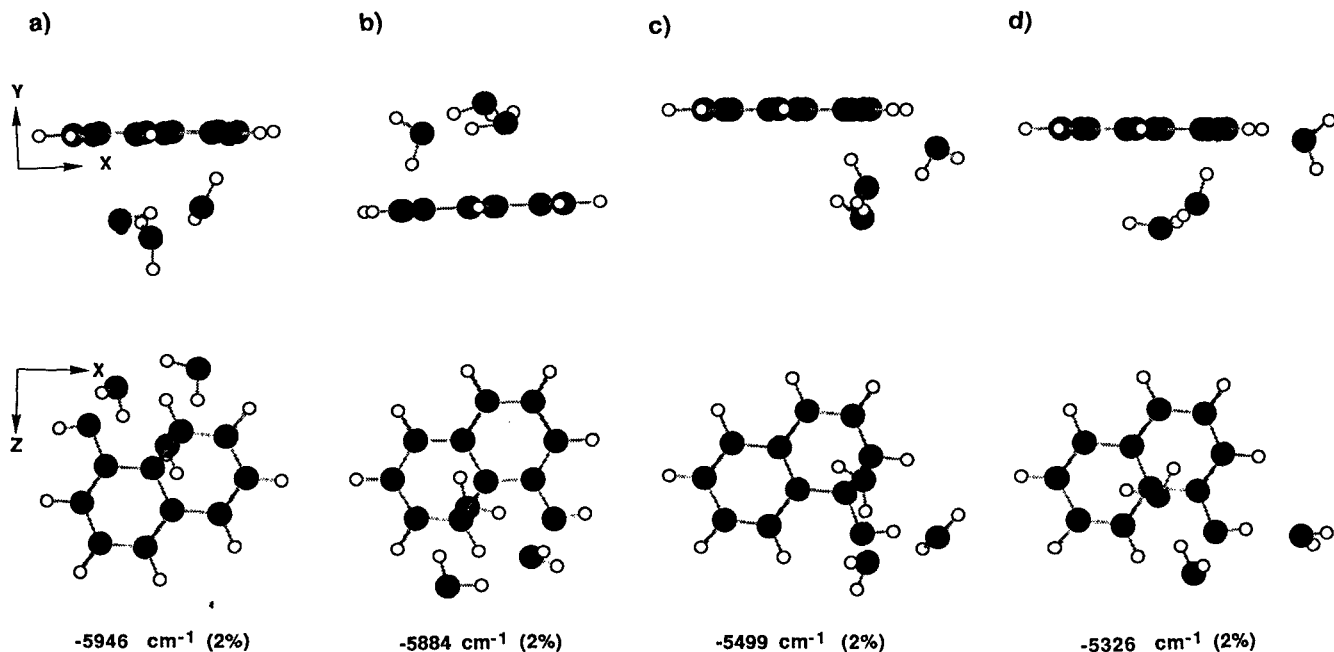-5946 cm⁻¹ (2%)   -5884 cm⁻¹ (2%)   -5499 cm⁻¹ (2%)   -5326 cm⁻¹ (2%)

FIG. 8. The four most stable geometries for 1-naphthol(H_2O)$_3$. The stabilization energy and the percentage of the total number of calculations resulting in the reported structure are indicated.

energetically favorable (by roughly a factor of 2). Similar trends are identified for 1-naphthol(H_2O)$_{3,4}$ clusters (Figs. 8 and 9). The waters all hydrogen bond together in the proximity of the solute OH group.

3. 1-Naphthol(NH₃)₁

The calculated geometries for ammonia clusters are quite different from those for water clusters. Figure 10 presents the 1-naphthol(NH₃)₁ cluster geometries. Here the

lowest energy clusters show a mixture of NH_3-π-system coordination and hydrogen bonding (ammonia hydrogen to naphtholic oxygen). This is consistent with and emphasizes the commonly held notion that O–H hydrogen bonding is stronger than N–H hydrogen bonding. The direction of the relatively weak naphthol/NH_3 hydrogen bonding is sensitive to the value of the atomic charges employed and the details of the chosen potential energy form. For example, Hartree–Fock rather than MOPAC 5 derived atomic charges reverse the hydrogen bond direction: nonetheless,
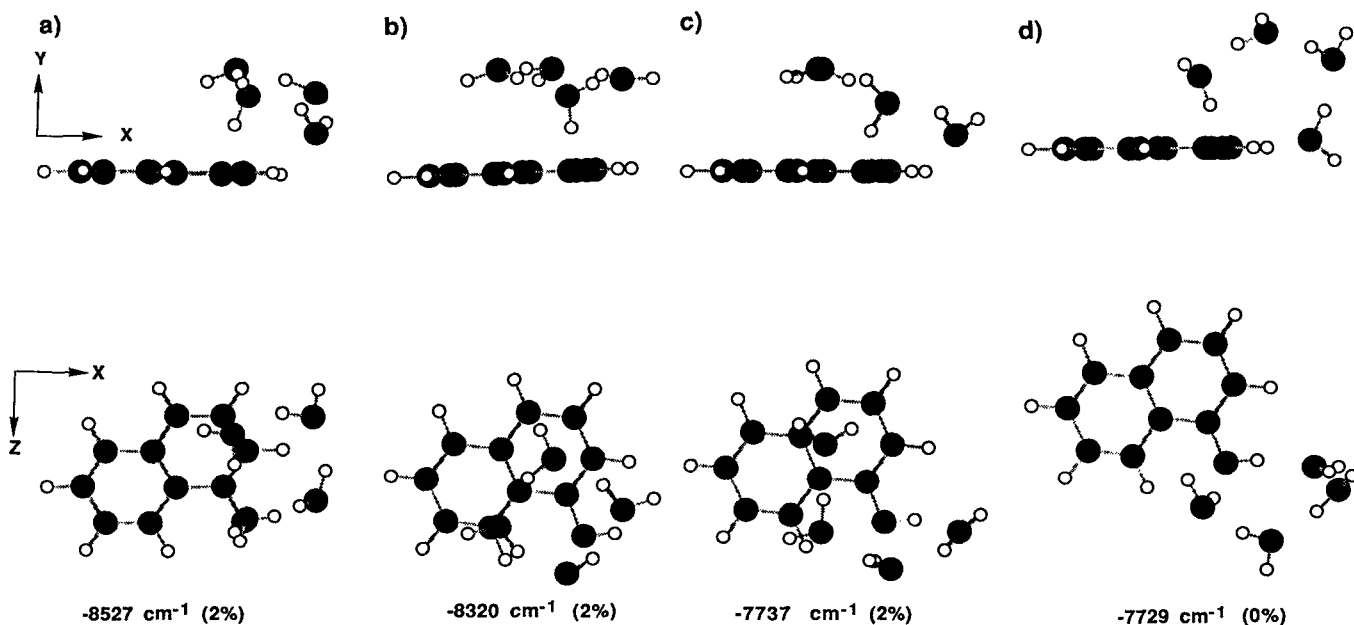
a)

b)

c)

d)

-8527 cm⁻¹ (2%)   -8320 cm⁻¹ (2%)   -7737 cm⁻¹ (2%)   -7729 cm⁻¹ (0%)

FIG. 9. The four most stable geometries for 1-naphthol(H_2O)$_4$. The geometry in (d) is calculated with one of H_2O molecule forced to make hydrogen bonding. The stabilization energy and the percentage of the total number of calculations resulting in the structure are indicated.
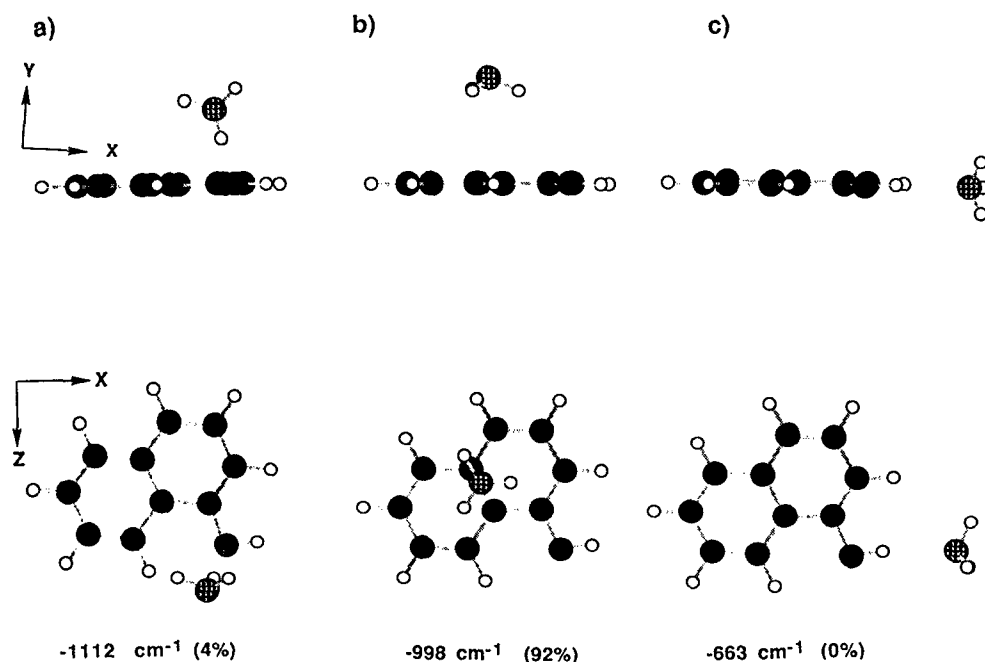
a)   b)   c)

-1112 cm⁻¹ (4%)   -998 cm⁻¹ (92%)   -663 cm⁻¹ (0%)

FIG. 10. (a) and (b) The two most stable geometries for 1-naphthol(NH$_3$)$_1$. The geometry in (c) is achieved only if the starting geometry is chosen to favor hydrogen bonding. The stabilization energy and the percentage of the total number of calculations resulting in the reported structure are indicated.

the comparison between naphthol/H$_2$O and naphthol/NH$_3$ cluster structure remains valid.

4. 1-Naphthol(NH$_3$)$_{2,3,4}$

The trend for large ammonia clusters is also somewhat different from that found for the larger water clusters: hydrogen bonding is emphasized to a much smaller extend and NH$_3$-π-system interactions become dominant. Since the NH$_3$–NH$_3$ interaction energy is smaller than the NH$_3$-1-naphthol interaction energy (~430 vs 1100 cm^{-1} for the potentials employed here) the ammonia molecules do not necessarily bond together, but rather occupy positions that distribute them about the 1-naphthol solute: that is, the ammonia molecules better solvate the 1-naphthol solute. The

general interaction, as can be seen readily in Figs. 11, 12, and 13, however, takes place with a bias toward the OH portion of the 1-naphthol.

IV. DISCUSSION

A. Threshold photoionization

The threshold photoionization spectra recorded in Fig. 4 and summarized in Table I separate the 1-naphthol water and ammonia clusters into three groups: (1) 1-naphthol (H$_2$O)$_n$, $n = 1,...,4$ with ionization threshold ~59 000 ± 200 cm^{-1}; (2) 1-naphthol(NH$_3$)$_{1,2}$ and most of the 1-naphthol(NH$_3$)$_3$ conformers with ionization threshold ~57 500 ± 200 cm^{-1}; and (3) one of the 1-naphthol(NH$_3$)$_3$ conformers and all 1-naphthol(NH$_4$)$_n$,

a)   b)   c)

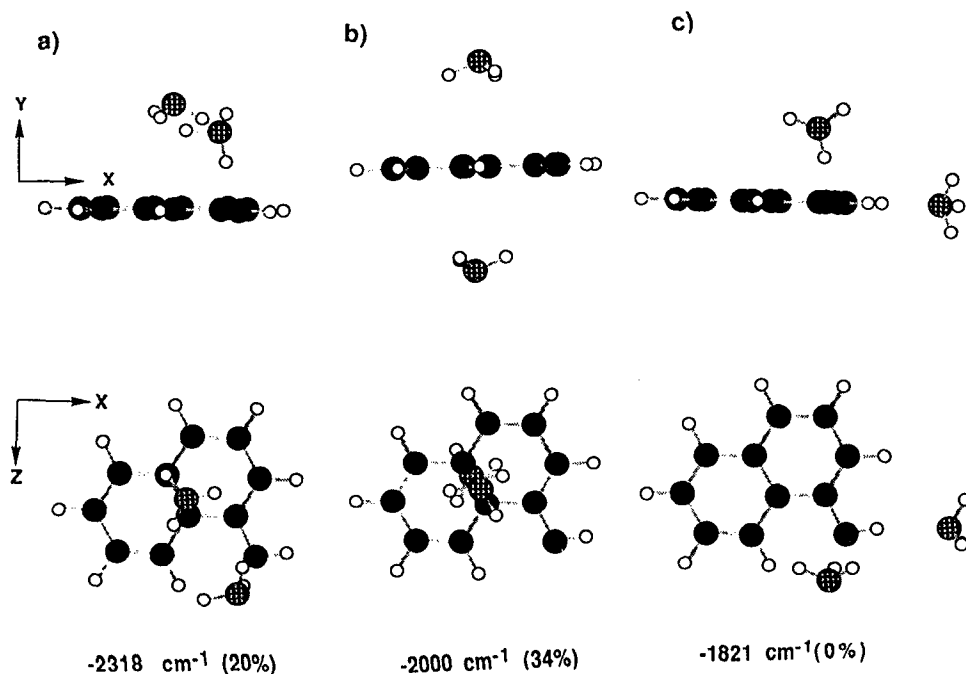-2318 cm⁻¹ (20%)   -2000 cm⁻¹ (34%)   -1821 cm⁻¹(0%)

FIG. 11. (a) and (b) The two most stable geometries for 1-naphthol(NH$_3$)$_2$. The geometry in (c) is calculated only if one NH$_3$ is forced into a hydrogen bonding structure. The stabilization energy and the percentage of the total number of calculations resulting in the reported structure are indicated.

-3500 cm⁻¹ (21%)   **-3470 cm⁻¹ (2%)**   **-3328 cm⁻¹ (17%)**   **-3038 cm⁻¹ (0%)**

FIG. 12. (a), (b), (c) The three most stable geometries for 1-naphthol(NH_3)$_3$. The geometry in (d) is calculated only if one NH_3 is forced into a hydrogen bonding structure. The stabilization energy and the percentage of the total number of calculations resulting in the reported structure are indicated.
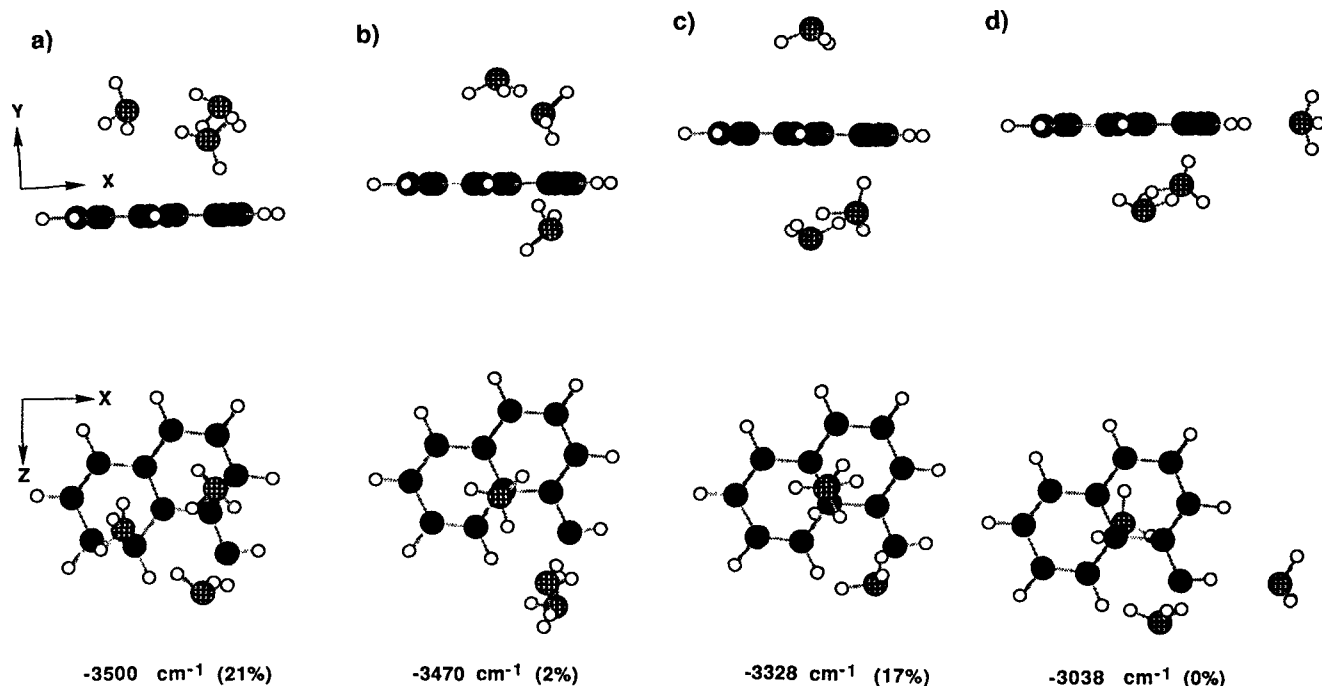
$n \geqslant 4$, conformers with ionization thresholds $\sim 56\,000\,\mathrm{cm}^{-1}$. The ionization threshold red shifts for the first two groups of clusters simply reflects the binding energy differences between the neutral ground state and the ion (~ 2500 and 4000 cm^{-1}, respectively). By way of comparison, the ionization potentials for the clusters indole(H_2O)$_1$ and (NH_3)$_{1,2}$, for

which no proton transfer has been characterized, are red shifted from the indole ionization potential by 3000, 4150, and 4550 cm^{-1}, respectively.[24]

In contrast, the large relative shift for the third grouping of clusters ($\sim 6650\,\mathrm{cm}^{-1}$) seems to suggest that proton transfer has occurred in these S_1 excited state systems. Per-

-4666 cm⁻¹ (8%)   **-4582 cm⁻¹ (2%)**   **-4200 cm⁻¹ (32%)**   **-4245 cm⁻¹ (0%)**
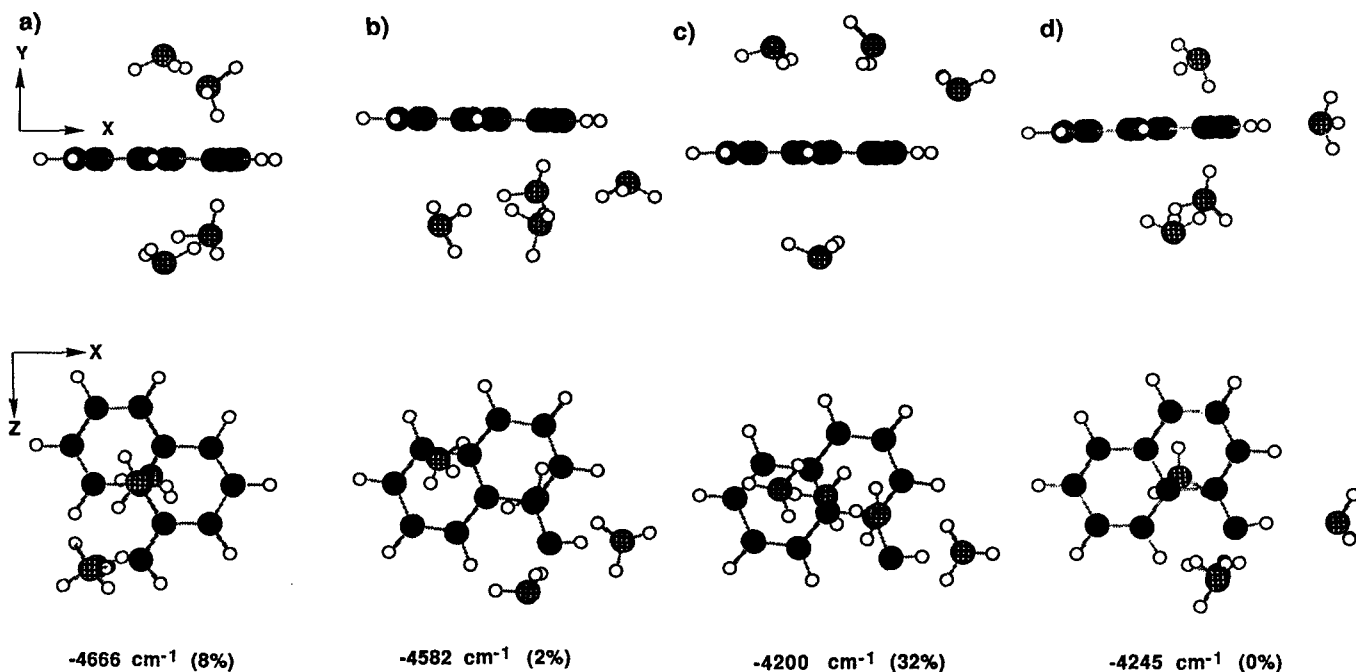
FIG. 13. (a), (b), (c) The three most stable geometries for 1-naphthol(NH_3)$_4$. The geometry in (d) is calculated only if one NH_3 is forced into a hydrogen bonding structure. The stabilization energy and the percentage of the total number of calculations resulting in the reported structure are indicated.

TABLE I. Summary of threshold photoionization for 1-naphthol and its NH_3 and H_2O clusters.

Sample	Excitation frequency (ν_{ex}, cm^{-1})	$I \leftarrow S_1$ threshold (ν_{ion}, cm^{-1})	Ionization potential (I.P.) ($\nu_{ex} + \nu_{ion}$, cm^{-1})	Shift of I.P. from bare molecular I.P. (cm^{-1})
1-naphthol	31 458	31 130 ± 3	62 588 ± 3	0
1-naphthol(H_2O)$_1$	31 310	27 680 ± 50	58 990 ± 50	−3598
1-naphthol(NH_3)$_1$	31 221	26 420 ± 50	57 641 ± 50	−4947
1-naphthol(NH_3)$_2$	31 105	26 460 ± 50	57 525 ± 50	−5063
1-naphthol(NH_3)$_3$	31 047	26 350 ± 80	57 397 ± 80	−5191
1-naphthol(NH_3)$_3$	31 068	> 26 420	> 57 488	> −5100
1-naphthol(NH_3)$_3$	31 105	24 840 ± 50	55 944 ± 50	−6644
1-naphthol(NH_3)$_4$	30 877	24 990 ± 50	55 867 ± 50	−6721
1-naphthol(NH_3)$_5$	30 877	< 24 520	< 55 408	< −7180

haps the major advantage of threshold photoionization studies over the dispersed emission studies of proton transfer is that the ionization studies employ mass resolution. Each technique has limitations with regard to selectivity, sensitivity, and interpretation, especially near the limits of the techniques [i.e., $(NH_3)_3$ vs $(NH_3)_4$ clusters]; however, the confluence of the three techniques, threshold ionization, dispersed emission, and time resolved, all yielding similar results is indeed compelling.

B. Comparison with previous results

All results for proton transfer in 1-naphthol(NH_3)$_n$, $n > 4$, and 1-naphthol(H_2O)$_n$, $n = 1, ... > 20$, agree: proton transfer in S_1 occurs in the first instance but not the second. We believe that our observations of conformers of different behavior for 1-naphthol(NH_3)$_3$ clusters help resolve the differences between the two previous[6,8] (dynamic and static) studies on this system. As shown in Fig. 3, the feature at ~31 105 cm^{-1} for 1-naphthol(NH_3)$_3$ has a very small intensity which is mostly masked in the one-color spectrum by high intensity species. Assuming that the transition probabilities for the $S_1 \leftarrow S_0$ and $I \leftarrow S_1$ steps of the neutral clusters are similar for these origin features, two explanations for the reduced intensity of the 31 105 cm^{-1} feature are plausible: (1) the population of this conformer is low; and (2) the S_1 lifetime and the ionization cross section for this cluster are reduced due to the $AH*(B_n) \rightarrow A*^-(HB_n)^+$ proton transfer reaction. Both mechanisms are possible and may well contribute to the reduced intensity of this conformer of 1-naphthol(NH_3)$_3$. The unfortunate overlap between a strong 1-naphthol(NH_3)$_2$ and a very weak 1-naphthol(NH_3)$_3$ transition probably explains why this feature has not been previously identified in dispersed emission proton transfer studies.[6] Of course, for picosecond time resolved studies, this 1-naphthol(NH_3)$_3$ conformer should be a dominant feature due to its greater concentration than $n > 4$ clusters and its time dependent mass detected signal.

C. Cluster structure calculations

Proton affinity of the solvent and stabilization (solvation) of the produced ions (A^-* and H^+) are two essential factors for the occurrence of excited state proton transfer reactions in clusters. The calculated cluster structures re-

ported in the last section can aid in the understanding of the effect of solute/solvent geometry on the proton transfer reaction. While the calculations are certainly potential and atomic charge dependent and the one employed here is certainly arbitrary and surely only qualitative, the calculated relative cluster trends are probably useful and indicative of the actual cluster behavior. Employing reasonable potentials should certainly generate cluster structures that embody the current state of knowledge of intermolecular interactions.

As shown in Figs. 6–9, 1-naphthol(H_2O)$_n$ clusters achieve low energy structures that emphasize hydrogen bonding between all the molecules, especially the water molecules: the water molecules thus have a tendency (for the large binding energy cluster structures) to bind together and reside as a group in the vicinity of the 1-naphthol OH group. Therefore, the solvation of the naphthalene portion of the naphthol molecule tends to be poor and somewhat incomplete even for clusters with large amounts of solvent waters ($n > 5$).

The calculations suggest the opposite trend for 1-naphthol(NH_3)$_n$ clusters. Hydrogen bonding is much less emphasized for these clusters and the NH_3–NH_3 interaction is small. Consequently, the ammonia molecules solvate both the OH and the aromatic moieties to a larger extent than found for the water solvent system even in small clusters. In addition, the probability for forming hydrogen bonded (O–H...NH_3) structures seems to increase as the clusters become larger ($n = 3, 4$) in this system as suggested in Figs. 11 and 12. While at first consideration this trend may be unexpected, note that the calculated ammonia benzene interaction is substantial (~600 cm^{-1}) and that 1-naphthol is not very acidic in its ground electronic state. The two competing interactions (dispersion and hydrogen bonding) then generate what might be called intermediate structures for which neither extreme bonding interaction dominates the calculated "compromise" structure.

Thus, the experimental and calculational results seem to imply for these cluster systems the following characterization: (1) in 1-naphthol(H_2O)$_n$ the proton transfer reaction does not occur because the proton affinity of water is low and because the naphtholate anion is not well stabilized or solvated by the water; and (2) in 1-naphthol(NH_3)$_n$ clusters the solvation of both the proton and the naphtholate anion is good for relatively low solvent number ($n \sim 3$–4) and the

ammonia proton affinity (although not necessarily hydrogen bonding preference or tendency) is relatively high. Cluster geometry and solvation structure at the margin of adequate solvation number seem to be an essential feature for the proton transfer reaction.

These above results are consistent with the time resolved matrix isolation studies of Ref. 25 which find rapid (<20 ps) proton transfer for 1-naphthol$(NH_3)_3$ clusters in an argon matrix.[25] Nonetheless, due to differences in solvation character, cluster structure, and Franck–Condon factors for absorption and proton transfer, the gas phase and matrix isolation cluster data need not be the same.

V. CONCLUSIONS

Based on threshold photoionization and dispersed emission data, we conclude that excited state proton transfer occurs in 1-naphthol/ammonia clusters for all $n \geqslant 4$ cluster conformations and (at least) one $n = 3$ cluster conformation. For all other ammonia and water clusters of 1-naphthol, no excited state proton transfer can be characterized. These results can be qualitatively rationalized on the basis of cluster structure and binding energy calculations employing a Lennard-Jones 6-12-1 potential form with hydrogen bonding (10-12-1) as appropriate. Calculations suggest that proton transfer is induced only if both proton and anion can be well solvated: for ammonia this occurs around $n = 3$ or 4 solvent molecules (depending on cluster geometry) because ammonia has a reduced (with respect to water) specific hydrogen bonding interaction, a relatively weak $NH_3–NH_3$ interaction, and an increased (with respect to water) cluster proton affinity.

[1] See papers in special issue for "Spectroscopy and Dynamics of Elementary Proton Transfer in Polyatomic Systems," in Chem. Phys. **136** (1989).
[2] *Atomic and Molecular Clusters*, edited by E. R. Bernstein (Elsevier, Amsterdam, 1990).
[3] T. Förster, Z. Elektrochem. **54**, 531 (1950).
[4] J. F. Ireland and P. A. H. Wyatt, Adv. Phys. Org. Chem. **12**, 131 (1976).
[5] O. Cheshnovsky and S. Leutwyler, Chem. Phys. Lett. **121**, 1 (1985).
[6] O. Cheshnovsky and S. Leutwyler, J. Chem. Phys. **88**, 4127 (1988).
[7] R. Knochenmuss, O. Cheshnovsky, and S. Leutwyler, Chem. Phys. Lett. **144**, 317 (1988).
[8] J. J. Breen, L. W. Peng, D. M. Willberg, A. Heikal, P. Cong, and A. H. Zewail, J. Chem. Phys. **92**, 805 (1990).
[9] T. Dorz, R. Knochenmuss, and S. Leutwyler, J. Chem. Phys. **93**, 4520 (1990).
[10] D. Solgadi, C. Jouvet, and A. Tramer, J. Phys. Chem. **92**, 3313 (1988).
[11] J. Steadman and J. A. Syage, J. Chem. Phys. **92**, 4630 (1990).
[12] C. Jouvet, C. Lardeux-Dedonder, M. Richard-Viard, D. Solgadi, and A. Tramer, J. Phys. Chem. **94**, 5041 (1990).
[13] M. R. Nimlos, D. F. Kelley, and E. R. Bernstein, J. Phys. Chem. **93**, 643 (1989).
[14] N. P. Ernsting, J. Phys. Chem. **89**, 4932 (1985); N. P. Ernsting, J. Am. Chem. Soc. **107**, 4564 (1985).
[15] S. K. Kim, S. -C. Hsu, and E. R. Bernstein, J. Chem. Phys. **95** (1991).
[16] N. Mikami, I. Suzuki, and A. Okabe, J. Phys. Chem. **91**, 5242 (1987).
[17] R. Knochenmuss and S. Leutwyler, J. Chem. Phys. **91**, 1268 (1989).
[18] E. R. Bernstein, K. Law, and M. Schauer, J. Chem. Phys. **80**, 207 (1984).
[19] G. Nemethy, M. S. Pottle, and H. A. Scherga, J. Phys. Chem. **87**, 188 (1983); F. A. Momany, L. M. Carruthers, R. F. McGuire, and H. A. Scherga, *ibid.* **78**, 1595 (1974).
[20] J. J. P. Stewart, J. Comput. Chem. **10**, 209, 221 (1989).
[21] J. M. Hollas and M. Z. B. Hussein, J. Mol. Spectrosc. **127**, 497 (1988).
[22] C. Lakshminarayan and J. L. Knee, J. Phys. Chem. **94**, 2637 (1990).
[23] J. R. Johnson, K. D. Jordan, D. F. Plusquellic, and D. W. Pratt, J. Chem. Phys. **93**, 2258 (1990).
[24] J. Hager, M. Ivanco, M. A. Smith, and S. C. Wallace, Chem. Phys. **105**, 397 (1986).
[25] G. A. Brucker and D. F. Kelley, J. Chem. Phys. **90**, 5243 (1989); Chem. Phys. **136**, 213 (1989).